Finite Element Analysis of a Six-Component Force Sensor for the Trans-Femoral Prosthesis

Xiao Hu, Rencheng Wang, Fangfang Wu, Dewen Jin, Xiaohong Jia, Jichuan Zhang, Fuwen Cai, and Shuangxi Zheng

Division of Intelligent and Biomechanical System
State Key Laboratory of Tribology, Tsinghua University Beijing, 100084, China
wangrc@mail.tsinghua.edu.cn

Abstract. It is significant to detect and analyze its mechanical property for the design of the artificial knee joint, especially for the design of an osseointegrated prosthetic limb. Since normal six-component force sensors are unsuitable for detecting the mechanical property of the lower limb prosthesis, a novel sensor is presented in this paper. It can be easily fixed between the artificial knee joint and the stump of the patient to detect the load condition during walking. The mathematic model of the sensor is analyzed, and strength check, stiffness design and the linearity of the sensor were studied with FEA. Finally, the Transmission Matrix is calculated. This kind of sensor can help us to get academic foundations for the designment and the evaluation of the limb prosthesis and its performance.

Keywords: Six-component force sensor, Prosthesis, FEA.

1 Introduction

Due to the complex load conditions of the lower limb prosthesis during walking, it is significant to detect and analyze its mechanical property for the design of the artificial knee joint, especially for the design of an osseointegrated prosthetic limb, which is implanted directly to the bone of the stump without socket [1][2]. The sensor used to detect the mechanical stress for prosthetic limb necessarily requires relatively great measuring range and should be easy to link to the artificial joint and the stump. However, the present six-component sensors have not enough range [3][4], or are too complicated to be utilized to detect the load of the lower prosthesis limb [5][6]. Moreover, most of these sensors are typically used in robotics and other industrial applications where a large mass is often not as much of a concern as in prosthetics applications [7]. Hence a special six-component force sensor is designed in this paper to meet such requirements.

2 Sensor Structure and Mathematic Model

The arrangement of strain gages on the elastic body of the sensor is shown in the Fig. 1. Six pairs of strain gages are stuck to the outer surface of the cylinder

V.G. Duffy (Ed.): Digital Human Modeling, HCII 2007, LNCS 4561, pp. 633–639, 2007.

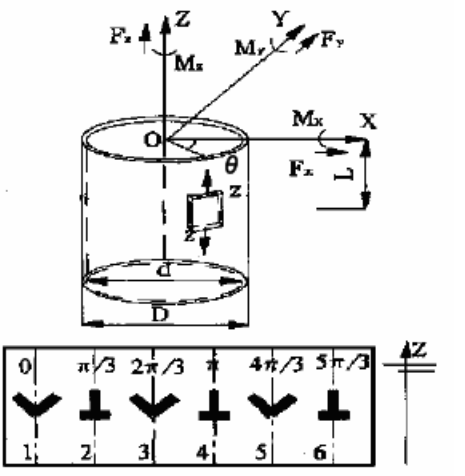

Fig. 1. Arrangement of strain gages on the elastic body

equidistantly. Each pair of strain gages is composed of two single perpendicular gages. The 1st, 3rd and 5th pairs of gages are used to detect the shearing strain. And the 2nd, 4th and 6th pairs are used to detect the normal strain. When the elastic body is deforming, according to the principle of superposition, we can derive the relationship between stress and each component of 6-axis forces.

The relationship of normal stress and relevant components of 6-axis forces is:

$$\sigma_{Z1} = -\left(F_X L\cos\theta\right)/W_X \tag{1}$$

$$\sigma_{Z2} = -\left(F_Y L\sin\theta\right)/W_X \tag{2}$$

$$\sigma_{Z3} = \left(M_X L\sin\theta\right)/W_X \tag{3}$$

$$\sigma_{Z4} = -\left(M_Y L\cos\theta\right)/W_X \tag{4}$$

$$\sigma_{Z5} = -F_Z/S \tag{5}$$

Where $W_X = \pi\left(D^4 - d^4\right)/32D$ is the section modulus in bending, $S = \pi\left(D^2 - d^2\right)/4$ is the cross-section area of the elastic body, D is the outer diameter of the elastic body and d is the inner diameter, L and θ are shown in the Fig. 1.

The shearing stress of the element can be caused by F_x, F_y, M_z, and the relationships are shown below:

$$\tau_{Fy} = \left(F_Y \cos^2 \theta\right)/S \tag{6}$$

$$\tau_{Fx} = \left(F_X \sin^2 \theta\right)/S \tag{7}$$

$$\tau_{Fy} = M_Z / B \tag{8}$$

Where $B = S\left(D + d\right)/2$.

From (1) ~ (8), it could be derived the relationship between the output voltage of the six pairs of strain gages and the 6-axis forces:

$$U=KC'F=CF \tag{9}$$

Where $U=\left[U_1, U_2, U_3, U_4, U_5, U_6\right]^T$ is output voltage of the six pairs of strain gages, $F=\left[F_1, F_2, F_3, M_1, M_2, M_3\right]^T$ is the 6-axis forces, K is the gage and bridge gain, which is a diagonal matrix, and C is the Transmission Matrix of the sensor, which is defined as (10) following:

$$C=\begin{bmatrix} 0 & \frac{K_1}{SG} & 0 & 0 & 0 & \frac{K_1}{BG} \\ -\frac{K_2 L}{2W_x E} & -\frac{\sqrt{3}K_2 L}{2W_x E} & -\frac{K_2}{SE} & \frac{\sqrt{3}K_2 L}{2W_x E} & -\frac{K_2 L}{2W_x E} & 0 \\ -\frac{3K_3}{4SG} & -\frac{K_3}{4SG} & 0 & 0 & 0 & \frac{K_3}{BG} \\ \frac{K_4 L}{W_x E} & 0 & -\frac{K_4}{SE} & 0 & \frac{K_4}{W_x E} & 0 \\ \frac{3K_5}{4SG} & -\frac{K_5}{4SG} & 0 & 0 & 0 & \frac{K_5}{BG} \\ -\frac{K_6 L}{2W_x E} & \frac{\sqrt{3}K_6 L}{2W_x E} & -\frac{K_6}{SE} & -\frac{\sqrt{3}K_6 L}{2W_x E} & -\frac{K_6 L}{2W_x E} & 0 \end{bmatrix} \tag{10}$$

Where E is the modulus of elasticity, and G is the shearing modulus.

3 Finite Element Analysis

3.1 Sensor Performance

The sensor was modeled as commercially 40Cr with elastic modulus of 210GPa and a Poisson's ratio of 0.28. The wall thickness of the elastic body is 1mm and its length is

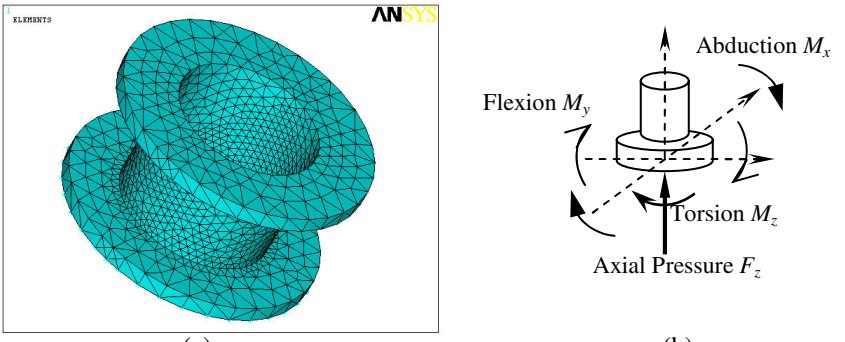

Fig. 2. Sensor model and applied loads

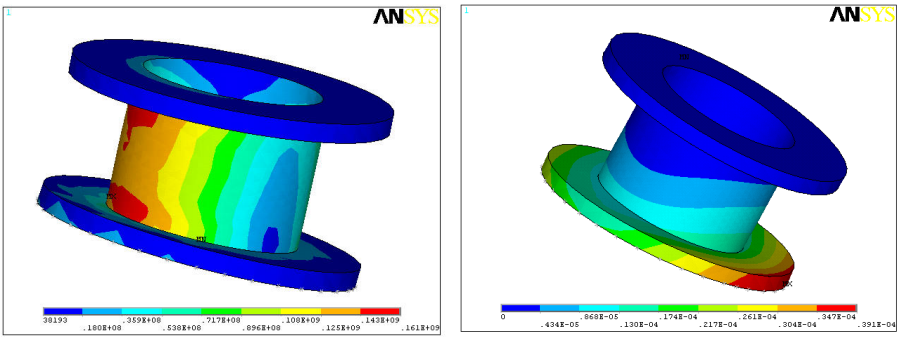

Fig. 3. Sensor contour maps of von Mises stress and deflection

20mm. The ANSYS FE package was used for stress and strain analysis. Simplified three-dimensional model of the sensor was developed using eight-noded axisymmetric harmonic elements (SOLID45), shown in Fig. 2(a). The model was free meshed. A total number of 6294 solid elements were generated to simulate the structure of the sensor. As shown in Fig. 2(b), a combination of axial compressive forces (F_y=3750N), torsion (M_z=20Nm), flexion (M_x=60Nm) and abduction (M_y=40Nm) bending moments load cases were applied to the models for the following investigation [8].

Fig. 3(a) shows the von Mises stress of the elastic body of sensor under the applied forces. The maximal stress of the model is 161MPa, which is less than the allowable stress of 40Cr (230MPa). Fig. 3(b) also shows the deflection of the sensor under the same condition. The maximal deflection is 39.1um, which has no negative effects on the sensor structure, so that the sensor can be safely used on the prosthesis. Therefore, it can be concluded that the material 40Cr is qualified in the sensor design.

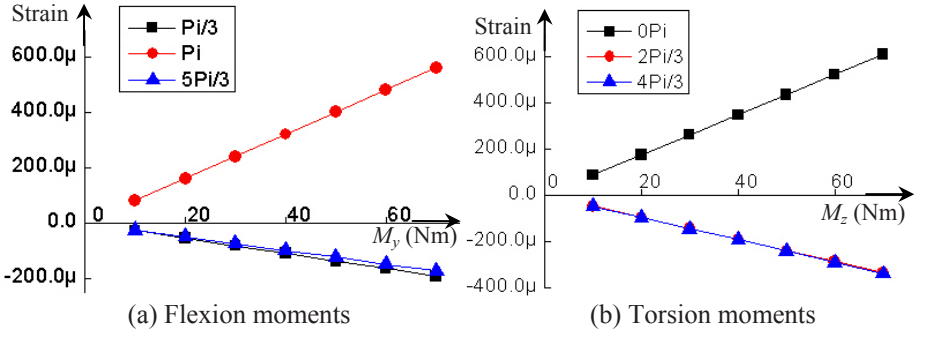

Fig. 4. Sensor linearity under flexion and torsion moments

The strain gages would be stuck on the middle of the sensor cylinder, 10mm from each end. With ANSYS, on those positions the gages would be stuck, the linearity of the sensor during the full measure range could be studied. In the full range of flexion and torsion moment (0~70Nm), we apply seven flexion moments to the sensor, each with an increment of 10Nm. The results are shown in the Fig. 4. The gage poison is shown with angle, Pi/3, Pi, etc. Other applied conditions also show the same results, but can not be indicated here due to the abstract length limitation.

3.2 Transmission Matrix of the Sensor

From (9), it could be derived:

$$F=C^{-1}U=C^{*}U \tag{11}$$

Where C^{*} is called the Transmission Matrix of the sensor.

According to (9), it can be derived that:

$$C^{*}=(C')^{-1}K^{-1} \tag{12}$$

So, (11) could be transformed as:

$$F=C^{*}U=(C')^{-1}K^{-1}U=(C')^{-1}S=C_1'S \tag{13}$$

The Eq. (9) could be transformed as:

$$S=C'F \tag{14}$$

Where S is the strains of the key points where the six pairs of gages are stuck. Eq. (13) and (14) indicates the relationship between the strain of gages and the forces applied to the sensor.

Since $C^{*}=(C')^{-1}K^{-1}=C_1'K^{-1}$ and $C=C'K$, the Transmission Matrix and Calibration Matrix could be studied preliminarily with C'. With ANSYS, six loads were respectively applied to the model of the sensor (Table 1). The strains of the key point could be obtained with ANSYS simulation.

Table 1. Six loads applied to the sensor model

Shear Force (F_x, N)	Shear Force (F_y, N)	Axial Pressure (F_z, N)	Abduction (M_x, Nm)	Flexion (M_y, Nm)	Torsion (M_z, Nm)
1000	1000	2000	50	50	50

With the simulation results, the C' could be obtained:

$$C'=1.0e\text{-}5\bullet\begin{bmatrix} 0.0000 & 0.0262 & 0.0000 & -0.0037 & 0.0174 & 0.9294 \\ -0.0048 & -0.0082 & -0.0053 & 0.6283 & -0.3721 & 0.0011 \\ -0.0109 & -0.0064 & -0.0000 & -0.0013 & -0.0003 & 0.9452 \\ 0.0093 & 0.0000 & -0.0049 & -0.0057 & 0.7026 & 0.0007 \\ 0.0118 & -0.0070 & 0.0000 & 0.0003 & 0.0058 & 0.9356 \\ -0.0047 & 0.0081 & -0.0049 & -0.6177 & -0.3436 & -0.0009 \end{bmatrix} \tag{15}$$

Compared with the theoretic Eq. (10), the main features are the same. Every column relates to one component of 6-axis forces applied to the sensor. For example, the first column relates to F_x, the fourth column relates to M_x, etc. Then, the Transmission Matrix could be obtained:

$$C^*=(C')^{-1}K^{-1}=1.0e6\bullet\begin{bmatrix} 0.0821 & 0.0232 & -4.4398 & -0.0103 & 4.4040 & 0.0351 \\ 3.0519 & 0.0289 & -1.5902 & -0.0423 & -1.4253 & 0.0142 \\ -0.0008 & -6.5710 & -0.0023 & -6.7181 & 0.0094 & -6.6208 \\ 0.0398 & 0.0775 & -0.0199 & -0.0005 & -0.0196 & -0.0833 \\ -0.0009 & -0.0459 & 0.0586 & 0.0952 & -0.0583 & -0.0477 \\ 0.0218 & 0.0004 & 0.0437 & -0.0005 & 0.0411 & 0.0002 \end{bmatrix}\bullet K^{-1} \tag{16}$$

When calibrating the sensor, the obtained theoretical Transmission Matrix could be used as a reference. However, due to the fabricating error and error caused by sticking the gages on the sensor, the practically observed value of C^* would deviate a little from the theoretical calculated value.

4 Conclusion

The sensor proposed in this paper is easy to link to the prosthesis, and strength check, stiffness design and the linearity of the sensor were studied with FEA. The results indicate the sensor could meet the requirements of the design and application.

Acknowledgement. This study is supported by a grant from the Chinese NSFC (№50475017).

References

1. Xu, W., Crocombe, A.D., Hughes, S.C.: Finite Element Analysis of Bone Stress and Strain around a Distal Osseointegrated Implant for Prosthetic Limb Attachment. Journal of Engineering in Medicine 6, 595–602 (2000)
2. Hsieh, M.C., Fang, Y.K., Ju, M.-S., Chen, G.-S., Ho, J.-J., et al.: A Contact-Type Piezoresistive Micro-Shear Stress Sensor for Above-Knee Prosthesis Application. IEEE Journal of Microelectromechanical Systems 1, 121–127 (2001)
3. Kim, G.-S.: The Design of a Six-Component Force/Moment Sensor and Evaluation of its Uncertainty. Meas. Sci. Technol. 9, 1445–1455 (2001)
4. Chao, L.-P., Chen, K.-T.: Shape Optimal Design and Force Sensitivity Evaluation of Six-Axis Force Sensors. Sens Actuators A Phys 2, 105–112 (1997)
5. Nishiwaki, K., Murakami, Y., Kagami, S., Kuniyoshi, Y., Inaba, M. et al.: A Six-Axis Force Sensor with Parallel Support Mechanism to Measure the Ground Reaction Force of Humanoid Robot. In: Proc IEEE Int Conf Rob Autom, pp. 2277–2282 (2002)
6. Liu, S.A., Tzo, H.L.: A novel six-component force sensor of good measurement isotropy and sensitivities. Sens Actuators A Phys 2-3, 223–230 (2002)
7. Sanders, J.E., Miller, R.A., Berglund, D.N., Zachariah, S.G.: Modular Six-Directional Force Sensor for Prosthetic Assessment: A Technical Note. J Rehabil Res. Dev. 2, 195–202 (1997)
8. Baumann, J.U., Schar, A., Meier, G.: Reaction Forces and Moments at Hip and Knee. In: Orthopade 1, 29–34 (1992)